We note that in the calculation of the vertical velocity field w, the individual modes are always continuous, since the integrals along the cuts contribute with the same sign when closing the contour of integration upward ($\xi < 0$) and downward ($\xi > 0$). In this case the branch points appear as pairs and the integrand is odd in μ. The above criterion cannot be used in this case.

LITERATURE CITED

1. J. B. Keller and W. H. Munk, "Internal wave wakes of a body moving in a stratified fluid," Phys. Fluids, 13, No. 6 (1970).
2. J. W. Miles, "Internal waves generated by a horizontally moving source," Geoph. Fluid Dyn., 2, No. 1 (1971).
3. V. F. Sannikov, "Near field of steady waves generated by a local source in a stratified fluid stream," in: Theoretical Studies of Wave Processes in the Ocean [in Russian], Sevastopol (1983).
4. V. E. Beven'kov and V. F. Sannikov, "Some features of the field of internal waves generated by a local source in a two-layer fluid stream," Zh. Prikl. Mekh. Tekh. Fiz., No. 2 (1987).
5. V. A. Borovikov, Yu. V. Vladimirov, and M. Ya. Kel'bert, "Field of internal gravitational waves generated by localized sources," Izv. Akad. Nauk SSSR, FAO, 20, No. 6 (1984).

TURBULENT FLOATING JET IN A STRATIFIED ATMOSPHERE

G. S. Golitsyn, Yu. A. Gostintsev, and A. F. Solodovnik

UDC 536.253

The reliability of predictions of the ecological consequences of a number of natural and anthropogenic catastrophes (volcano eruptions, large fires, atomic electric station emergencies, nuclear explosions) depends to a significant extent on the accuracy of predicting the initial spatial pattern of atmospheric pollution above individual heat and impurity sources [1]. The maximal altitude of impurity ejection and its concentration distribution in space at a time near to termination of average vertical freely convective movements of clouds or jets of heated products are understood to be the initial pollution.

Depending on the relationship between the time of heat (impurity) source action t_s and the characteristic time of thermal relaxation of the atmosphere $t_N \approx 2\pi N^{-1}$ (N is the Väisälä–Brunt frequency), two limiting spatial configurations of freely convective motions [2] can be separated out. If $t_s \ll t_N$ (in the limit for instantaneous energy liberation) then a floating cloud, a thermal, severed from the earth, is formed rapidly in the atmosphere. A convective column of an ascending jet movement of the products is formed above the focus for the reverse relationship between the times (in the limit for a permanently acting source). For the standard state of the atmosphere ($N = 0.0106$ sec^{-1} in the tropospheric layer) $t_N \approx$ 10 min. During this time the cloud or jet reaches its maximal point of ascent and starts to be deformed in mainly a horizontal direction. The thermal will here perform damping vibrational vertical motions around the thermal equilibrium level, while the convective column (from a fire focus, say) will form a slowly expanding configuration of a quasistationary jet flow at the altitude of hanging.

The transport of impurities in the atmosphere by powerful thermals is investigated in sufficient detail by both analytic [2-5] and numerical [6, 7] methods and the predictions of theory are mainly in good agreement with experimental results. Results of studying the second limit case of freely convective motions, the two-dimensional axisymmetric turbulent floating jet, are elucidated below.

Moscow. Translated from Zhurnal Prikladnoi Mekhaniki i Tekhnicheskoi Fiziki, No. 4, pp. 61-72, July-August, 1989. Original article submitted April 7, 1988.

0021-8944/89/3004-0566$12.50

FUNDAMENTAL EQUATIONS

The system of equations for the average parameters of a stationary turbulent freely convective axisymmetric jet in a stratified atmosphere in a boundary-layer approximation has the form [2, 4, 8]

$$\frac{\partial u^2}{\partial x}+\frac{1}{r}\frac{\partial}{\partial r}rvu=\frac{1}{r}\frac{\partial}{\partial r}\frac{\sigma\Psi_x}{r}\frac{\partial u}{\partial r}+\omega,$$
$$\frac{\partial}{\partial x}u\omega+\frac{1}{r}\frac{\partial}{\partial r}rv\omega=\frac{\mathrm{Pr}^{-1}}{r}\frac{\partial}{\partial r}\frac{\sigma\Psi_x}{r}\frac{\partial\omega}{\partial r}-uN^2,$$
$$\frac{\partial}{\partial x}u\vartheta+\frac{1}{r}\frac{\partial}{\partial r}rv\vartheta=\frac{\mathrm{Pr}^{-1}}{r}\frac{\partial}{\partial r}\frac{\sigma\Psi_x}{r}\frac{\partial\vartheta}{\partial r}-\frac{uN^2}{g\beta},$$
$$\frac{\partial}{\partial x}u\varepsilon_j+\frac{1}{r}\frac{\partial}{\partial r}rv\varepsilon_j=\frac{\mathrm{Sc}_j^{-1}}{r}\frac{\partial}{\partial r}\frac{\sigma\Psi_x}{r}\frac{\partial\varepsilon_j}{\partial r}-u\frac{d\varepsilon_{ja}}{dx},\quad \frac{\partial u}{\partial x}+\frac{1}{r}\frac{\partial}{\partial r}rv=0, \tag{1}$$
$$\omega=g\frac{\rho_a-\rho}{\rho_a}\approx g\left[\beta\vartheta+\frac{\mu_a}{\mu_b}\sum_{j=1}^{p}\varepsilon_j\left(\frac{\mu_b}{\mu_j}-1\right)\right],\quad \frac{\mu_a}{\mu_b}=\left[1+\sum_{j=1}^{k}\left(\frac{\mu_b}{\mu_j}-1\right)\varepsilon_{ka}\right]^{-1}.$$

Here x, r and $u=r^{-1}\dot{\Psi}_r$, $v=-r^{-1}\dot{\Psi}_x$ are the vertical and radial coordinates and the corresponding average velocity components; Ψ is the stream function; $\vartheta=T-T_a$ and $\varepsilon_j=c_j-c_{ja}$ are the excess values of the temperature and the mass concentration of the j-th impurity concentration (with molecular weight μ_j) in the jet with respect to their values in the atmosphere; $\beta\approx 1/T_a$ is the thermal coefficient of expansion; ω is the acceleration of the buoyancy force; and Pr and Sc_j are the turbulent analogs of the Prandtl and Schmidt numbers.

In the general case, an ascending jet consists of $1+p=1+k+m=1+\ell+n+m$ components, where the index 1 corresponds to dry air, ℓ to the impurity components contained in both the source and the atmosphere, m to just source components, and n to impurities in just the original atmosphere. The environment is formed by components $1+k=1+\ell+n$.

The Boussinesq hypothesis

$$\langle v',\ u'\rangle=-E\,\partial u/\partial r,\ \langle v'\vartheta'\rangle=-\mathrm{Pr}^{-1}E\,\partial\vartheta/\partial r,$$
$$\langle v'\varepsilon_j'\rangle=-\mathrm{Sc}_j^{-1}E\,\partial\varepsilon_j/\partial r,\ \langle v^{\ell}\omega^{\ell}\rangle=-\mathrm{Pr}^{-1}E\partial\omega/\partial r,$$

is used in deriving (1), where the semiempirical closure hypothesis

$$E=\frac{\sigma\Psi_x}{r^2}=\frac{\sigma x}{r^2}\int ur\,dr$$

justified earlier [4, 8] is taken for the turbulent kinematic viscosity E (σ is the dimensionless coefficient of turbulence determined experimentally).

The second equation in (1) for acceleration of the buoyancy force is obtained after multiplying the third equation by $(g\beta)$, each of the j fourth equations by $g\varepsilon_j(\mu/\mu_j-1)$, and adding them under the condition $\mathrm{Sc}_j=\mathrm{Sc}=\mathrm{Pr}$.

The square of the Väisälä–Brunt frequency

$$N^2=-g\left(\frac{d\ln\rho_a}{dx}+\frac{g}{c_s^2}\right)=\frac{g}{T_a}\left(\frac{dT_a}{dx}+\frac{g}{c_p}\right)\approx g\beta\left(\frac{dT_a}{dx}+\frac{g}{c_p}\right) \tag{2}$$

characterizes stratification of the environment. The value $g/c_p\approx 0.0098$ deg/m in (2) characterizes the adiabatic, and dT_a/dx the actual temperature gradient. For $N^2>0$ the atmosphere is stratified stable [in the International Standard Atmosphere (ISA) model for the troposphere to an altitude of ≈11 km we take $dT_a/dx=-0.0065$ deg/m = const, $\beta=1/288$ deg^{-1}, and $N=1.06\cdot10^{-2}$ sec^{-1}, while $N\approx 0.022$ sec^{-1} = const in the stratosphere to an altitude of ~40 km].

It is seen from (1) that the dynamic problem of a freely-convective jet in a stratified atmosphere under the assumptions made can be solved autonomously on the basis of just the continuity, motion, and buoyancy equations without detailing the temperature and concentration distributions.

SELF-SIMILAR FLOATING JET

For an irrespective stratified atmosphere (N = 0) or for relatively low rise altitudes when the penultimate term in the energy and buoyancy equations can be neglected, a self-similar motion mode holds as determined by just the conservation integrals of the system (1)

$$\int_0^\infty u\omega r\,dr = \int_0^\infty ug\frac{\Delta\rho}{\rho_a}r\,dr = \Pi_0, \quad \int_0^\infty u\vartheta r dr = Q_0. \tag{3}$$

The flux of the j-th gas component in the jet for invariability of the molecular composition of the atmosphere ($d\varepsilon_{k\,a}/dx = 0$) is also conserved

$$\int_0^\infty u\varepsilon_j r\,dr = P_{j0}. \tag{4}$$

The self-similar solution (1), (3), and (4) with the boundary conditions

$$\frac{\partial u}{\partial r} = v = \frac{\partial\omega}{\partial r} = \frac{\partial\vartheta}{\partial r} = \frac{\partial\varepsilon_j}{\partial r} = 0 \text{ for } r = 0,\ u = \omega = \vartheta = \varepsilon_j \to 0 \text{ for } r \to \infty$$

is sought among the functions

$$\begin{aligned}
&\Psi = (\Pi_0\sigma^2)^{1/3}x^{5/3}\varphi(\eta),\ u = (\Pi_0/\sigma)^{1/3}x^{-1/3}\varphi_3(\eta),\\
&v = (\Pi_0\sqrt{\sigma})^{1/3}x^{-1/3}\varphi_1(\eta),\ \omega = (\Pi_0/\sigma)^{2/3}x^{-5/3}f(\eta),\\
&\vartheta = Q_0(\Pi_0\sigma^2)^{-1/3}x^{-5/3}f(\eta),\ \varepsilon_j = P_{j0}(\Pi_0\sigma^2)^{-1/3}x^{-5/3}f(\eta),\\
&E = (\Pi_0\sigma^2)^{1/3}x^{2/3}\varphi(\eta)/\eta^2,\ \eta = r/(x\sqrt{\sigma}),\ \varphi_1 = \varphi' - 5/3\varphi/\eta,\\
&\varphi_3 = \varphi'/\eta.
\end{aligned} \tag{5}$$

For Sc_j = Sc = Pr there is similarity of the self-similar profiles of the excess concentration, temperature, and acceleration of the buoyancy force (density deficit in the jet).

For two cases (Pr = Sc_j = 0.6 and 2.0) there are analytic solutions of the self-similar system of equations [8]: for Pr = Sc = 0.6,

$$\begin{aligned}
&\varphi = \sqrt[3]{3}\,(1 - \exp(-\eta^2/2)),\quad \varphi_1 = \sqrt[3]{3}\left[\eta\exp(-\eta^2/2) - \right.\\
&\left. - \frac{5}{3\eta}(1 - \exp(-\eta^2/2))\right],\\
&\varphi_3 = \sqrt[3]{3}\exp(-\eta^2/2),\quad f = 2/\sqrt[3]{3}\exp(-\eta^2/2);
\end{aligned}$$

for Pr = Sc = 2,

$$\begin{aligned}
&\varphi = 3\sqrt[3]{0.03}\left(1 - \exp\left(-\frac{5}{6}\eta^2\right)\right),\quad \varphi_3 =\\
&= 5\sqrt[3]{0.03}\exp\left(-\frac{5}{6}\eta^2\right),\quad f = \frac{1}{\sqrt[3]{0.03}}\exp\left(-\frac{5}{6}\eta^2\right).
\end{aligned}$$

Results obtained by a numerical solution in the range of Pr = Sc values between 0.2 and 2 can be approximated by the functions

$$\begin{aligned}
&\varphi = A/m_0\exp(-m_0\eta^2),\ f = C\exp(-(5/6)\mathrm{Pr}\,\eta^2),\\
&A = 0.7443\,\mathrm{Pr}^{0.0618},\ C = 1.9821\,\mathrm{Pr}^{0.6993},\ m_0 = 1.4752\,\mathrm{Pr}^{0.7611} - (5/6)\mathrm{Pr}.
\end{aligned} \tag{6}$$

For Pr = Sc = 2, the effective dynamic boundary layer in a freely-rising turbulent jet is thicker than the thermal and concentrational, while for Pr = Sc = 0.6 total similarity of the profiles holds, and for Pr = Sc < 0.6 the vertical velocity profile is narrower than that for the heat and the concentration.

The dependences (6) permit determination of the value of Pr and the turbulence coefficient σ by means of the experimentally found profiles of the average temperature and the vertical velocity in an axisymmetric floating jet. Thus, the semiempirical expressions

$$u \approx 4.7(2\pi\Pi_0/x)^{1/3} \exp(-96r^2/x^2),\ g\beta\vartheta \approx 11x^{-5/3}(2\pi\Pi_0)^{2/3} \exp(-74\ r^2/x^2) \tag{7}$$

are proposed in [9] for the self-similar section of the freely-convective jet on the basis of processing test data. Comparing (7) with (5) and (6), we find the values of the parameters Pr = 0.46 and $\sigma \approx 6.6\cdot10^{-3}$ matching the theory to the profiles (7).

It should be noted that doubt is expressed in [3] about the validity of the representation of the experiments [9] by the dependences (7), which it is proposed to replace by

$$\begin{aligned} u &= k_1(2\pi\Pi_0/x)^{1/3} \exp(-80r^2/x^2), \\ g\beta\vartheta &= k_2x^{-5/3}(2\pi\Pi_0)^{2/3} \exp(-80\ r^2/x^2). \end{aligned} \tag{8}$$

The values Pr = 0.6, $\sigma = 6.25\cdot10^{-3}$ correspond to the profiles (8). Given for the self-similar section of the floating jet are the expressions

$$\frac{u_m}{u_0} = 3.5\,\mathrm{Fr}^{-1/3}\left(\frac{\rho_0}{\rho_a}\right)^{1/3}\left(\frac{x}{D_0}\right)^{-1/3},\quad \frac{T_m - T_a}{T_0 - T_a} = 8.22\,\mathrm{Fr}^{1/3}\left(\frac{\rho_0}{\rho_a}\right)^{-1/3}\left(\frac{x}{D_0}\right)^{-5/3}, \tag{9}$$

that approximate the experiments, where $\mathrm{Fr} = \rho_0u_0^2/[gD_0(\rho_a - \rho_0)]$ is the Froude number; u_m and T_m are the velocity and temperature on the jet axis; the subscript 0 denotes values of the initial jet parameters at the exit from a source with diameter D_0. Comparing (8) and (9) with the theoretical results of the present paper shows that to ±12% accuracy both series of experimental data are successfully matched for Pr = 0.61, σ = 0.0088 by the dependences

$$\begin{aligned} &\frac{u_m}{u_0} = 3.6\,\mathrm{Fr}^{-1/3}\left(\frac{\rho_0}{\rho_a}\right)^{1/3}\left(\frac{x}{D_0}\right)^{-1/3},\quad \frac{T_m - T_a}{T_0 - T_a} = 8.7\,\mathrm{Fr}^{1/3}\left(\frac{\rho_0}{\rho_a}\right)^{-1/3}\left(\frac{x}{D_0}\right)^{-5/3}, \\ &u = 3.9(2\pi\Pi_0/x)^{1/3} \exp(-70r^2/x^2),\ g\beta\vartheta = 10.2\ x^{-5/3} \times \\ &\times (2\pi\Pi_0)^{2/3} \exp(-70r^2/x^2). \end{aligned} \tag{10}$$

Floating jets possess an initial dynamic momentum near the source, while the velocity and excess temperature distributions in this section are described by forced convective flow regularities [11]

$$\frac{u_m}{u_0} \approx 6.6\left(\frac{\rho_0}{\rho_a}\right)^{1/2}\left(\frac{x}{D_0}\right)^{-1},\quad \frac{T_m - T_a}{T_0 - T_a} \approx 5.1\left(\frac{\rho_0}{\rho_a}\right)^{-1/2}\left(\frac{x}{D_0}\right)^{-1}.$$

Comparing these expressions with (10), the condition for realization of the self-similar ditributions inherent to a floating jet can be written

$$x/D_0 \geqslant 2.0\ \mathrm{Fr}^{1/2}(\rho_0/\rho_a)^{1/4}.] \tag{11}$$

FLOATING JET IN A STABLE ATMOSPHERE

The integrals (10) in the buoyancy and heat fluxes with respect to the jet altitude are not conserved for a stratified atmosphere and a self-similar mode is impossible in the whole domain of propagation. The vertical motion is retarded for stable stratification, the jet expands rapidly, and near the zeroth buoyancy level the gas rise practically ceases. Unstable atmosphere stratification contributes to flow acceleration [4].

The presence of a stratified environment is associated formally with the appearance of an additional governing parameter N with the dimensionality 1/sec in the original system of equations for the dynamic problem (the buoyancy flux integral Π_0 with the dimensionality m^4/sec^3 has the meaning of an initial condition in this case).

Since it is impossible to compile any dimensionless complex from the dimensional parameters mentioned, we then introduce the characteristic dimensionalities

$$\begin{aligned} &X_* = [\Pi_0/(\sigma N^3)]^{1/4},\quad R_* = X_*\sqrt{\sigma},\quad \Psi_* = X_*^3\sigma N, \\ &U_* = X_*N,\quad V_* = X_*N\sqrt{\sigma},\quad \Omega_* = X_*N^2. \end{aligned} \tag{12}$$

We seek the solution of (1) for the dynamic problem in the form

$$\Psi = \Psi_* \Phi(\eta, \zeta), \quad \omega = \Omega_* F(\eta, \zeta), \quad \eta = r/R_*, \quad \zeta = x/X_*. \tag{13}$$

Substituting (13) into (1) we obtain

$$\begin{gathered} \frac{\partial}{\partial \eta} \frac{\Phi}{\eta} \frac{\partial}{\partial \eta} \frac{1}{\eta} \frac{\partial \Phi}{\partial \eta} + \zeta \frac{\partial}{\partial \eta} \frac{\partial \Phi}{\partial \eta} \frac{\partial \Phi}{\partial \zeta} - \zeta^3 \frac{\partial}{\partial \zeta} \frac{1}{\eta \zeta^2} \left(\frac{\partial \Phi}{\partial \eta} \right)^2 + \eta \zeta^5 F = 0, \\ \mathrm{Pr}^{-1} \frac{\partial}{\partial \eta} \frac{\Phi}{\eta} \frac{\partial F}{\partial \eta} + \zeta \left(\frac{\partial}{\partial \eta} F \frac{\partial \Phi}{\partial \zeta} - \frac{\partial}{\partial \zeta} F \frac{\partial \Phi}{\partial \eta} \right) \mp \zeta \frac{\partial \Phi}{\partial \eta} = 0 \end{gathered} \tag{14}$$

with the boundary conditions in η

$$\varphi = (\Phi'/\eta)' = F' = 0 \text{ for } \eta = 0, \ \Phi'/\eta = F \to 0 \text{ for } \eta \to \infty.$$

The minus sign in the second equation in (13) corresponds to stable, and the plus to unstable stratification of the atmosphere. The quantity N in (12) is taken in absolute value for the second modification.

Analysis of (14) shows that for small ζ a self-similar solution exists to the accuracy of terms of order $\sim O(\zeta^{8/3})$, and which has the following form in the variables taken:

$$\Phi_0 = M_0 (1 - \exp(-m_0 \eta^2)) \zeta^{5/3}, \ F_0 = N_0 \exp(-k_0 \eta^2) \zeta^{-5/3}.$$

The values of the numerical coefficients M_0, m_0, N_0, and k_0 depend in a known manner on Pr (see the previous section).

The approximate solution of (14) for stable atmosphere stratification is sought by using the method of integral relations in a double series form

$$\begin{gathered} \Phi = \sum_{n=0} M_n [1 - \exp(-m_n \eta^2)] \zeta^{(8n+5)/3}, \quad m_n = \frac{m_0}{1+n}, \\ F = \sum_{n=0} N_n \exp(-k_n \eta^2) \zeta^{(8n-5)/3}, \ k_n = \frac{k_0}{1+n}, \quad n = 0, 1, 2, \ldots. \end{gathered} \tag{15}$$

that satisfy the boundary conditions in η.

Integrating (14) with respect to η between 0 and ∞ with the boundary conditions taken into account yields the integral equations

$$\frac{\partial}{\partial \zeta} \zeta^{-2} \int_0^\infty \frac{1}{\eta} \left(\frac{\partial \Phi}{\partial \eta} \right)^2 d\eta = \zeta^2 \int_0^\infty F \eta d\eta, \quad \frac{\partial}{\partial \zeta} \int_0^\infty F \frac{\partial \Phi}{\partial \eta} d\eta = -\Phi(\infty). \tag{16}$$

Substituting (15) into (16) permits finding the unknown coefficients M_n and N_n for values of M_0, m_0, N_0, k_0 known for the Pr selected and given m_n and k_n after terms with identical powers of ζ have been grouped. The first four values are presented in Table 1.

We write the vertical and radial velocity profiles in the dimensionless variables (13) as

$$\begin{gathered} \Phi_3 = 2 \sum_{n=0} M_n m_n \exp(-m_n \eta^2) \zeta^{(8n-1)/3}, \\ \Phi_1 = -\frac{1}{\eta \zeta} \sum_{n=0} \left| \left(\frac{8n+5}{3} \right) M_n (1 - \exp(-m_n \eta^2)) \zeta^{(8n+2)/3} - \right. \\ \left. - 2 M_n m_n \eta^2 \exp(-m_n \eta^2) \zeta^{(8n-1)/3} \right|. \end{gathered} \tag{17}$$

The dependences for relative values of the axial velocity and the density in the jet can also be represented in the parametric form

$$\begin{gathered} \frac{u}{u_0} = 2 \sum_{n=0} M_n m_n \mathrm{Fr}_1^{(2n-1)/3} \mathrm{Sh}^{2n} \hat{x}^{(8n-1)/3} \exp(-m_n \xi^2/\hat{x}^2), \\ \frac{\rho - \rho_a}{\rho_0 - \rho_a} = (8\sigma)^{-1} \sum_{n=0} N_n \mathrm{Fr}_1^{(2n+1)/3} \mathrm{Sh}^{2n} \hat{x}^{(8n-5)/3} \exp(-k_n \xi^2/\hat{x}^2), \end{gathered} \tag{18}$$

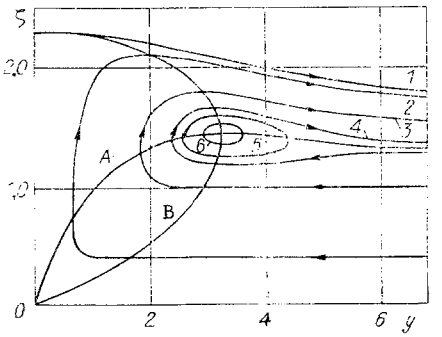

Fig. 1

TABLE 1

Pr=0,35		Pr=0,6		Pr=1	
$M_0 = 1{,}788;$	$m_0 = 0{,}3924$	1,44225;	0,5	1,204;	0,61
$M_1 = -0{,}3698;$	$m_1 = 0{,}1962$	−0,23401;	0,25	−0,1578;	0,305
$M_2 = -0{,}0410;$	$m_2 = 0{,}1308$	−0,02004;	0,1667	−0,0134;	0,1525
$M_3 = -0{,}0094;$	$m_3 = 0{,}0981$	−0,00349;	0,125	−0,0018;	0,1017
$N_0 = 0{,}9745;$	$k_0 = 0{,}2913$	1,38672;	0,5	1,965;	0,8333
$N_1 = -0{,}4023;$	$k_1 = 0{,}1456$	−0,45000;	0,25	−0,5151;	0,4167
$N_2 = -0{,}0025;$	$k_2 = 0{,}0971$	−0,00169;	0,1667	−0,0008;	0,2083
$N_3 = -0{,}0007;$	$k_3 = 0{,}0728$	−0,00032;	0,125	−0,00016;	0,1389
$\zeta_m = 1{,}89;$	$\zeta_m/\zeta_u = 1{,}24$	2,074;	1,24	2,284;	1,28
$\zeta_u = 1{,}52;$	$\zeta_\ell/\zeta_u = 0{,}74$	1,671;	0,74	1,78;	0,74
$\zeta_\ell = 1{,}13;$	$\zeta_1/\zeta_u = 0{,}91$	1,242;	0,91	1,32;	0,92
$\zeta_1 = 1{,}38;$	$\zeta_2/\zeta_u = 0{,}84$	1,515;	0,84	1,646;	0,83
$\zeta_2 = 1{,}28;$	$(\zeta_u - \zeta_\ell)/\zeta_2 = 0{,}3$	1,409;	0,3	1,485;	0,31

where $Fr_1 = \rho_a u_0^2 8\sigma/[g(\rho_a - \rho_0)D_0]$ and $Sh = ND_0/u_0$ are the modified Froude and Strouhal numbers; $\hat{x} = x/D_0$; $\xi = r/(D_0\sqrt{\sigma})$; u_0 and ρ_0 are the velocity and density in the source.

The flow field of a turbulent freely convective jet in a stably stratified atmosphere, computed on the basis of (15) and (17), is presented in Fig. 1 for Pr = 1 in the coordinates ζ, $y = r/(X_*\sqrt{\sigma})$. Lines 1-6 correspond to values of the dimensionless stream function Φ = 0, 0.26, 1.04, 1.27, 1.32, 1.37. The radial and vertical velocity components, respectively, equal zero on the lines A and B. It is seen that a freely-ascending jet reaches its highest point of rise $\zeta_m \approx 2.284$ on the axis. Here the gas is supercooled and heavier than the environment (the point of zeroth buoyancy is on the axis at $\zeta_1 = 1.646$); consequently, by spreading in the horizontal direction it subsides. Under stationary conditions, as $\xi \to \infty$, in the absence of vertical diffusion, the whole air mass attached to the floating jet near the base is removed radially from the axis with a horizontal layer between $\zeta_u \approx 1.78$ (the asymptotic coordinate of the line $\Psi = 0$ as $\xi \to \infty$) and $\zeta_\ell \approx 1.32$ (the asymptotic coordinate of the line $v = 0$ as $\xi \to \infty$). The level $\zeta_2 = 1.485$ is the zeroth value of the buoyancy flux integral $\int_0^\infty u\omega r dr = 0$. Near the intersection of the curves A (v = 0) and B (u = 0) there is a closed domain of vortex motion.

The computed values of the coordinates ζ_i of the characteristic points of the hanging jet are presented in Table 1. Despite the difference in the absolute values, their relative location is practically independent of Pr. For Pr = 0.06 the dependences

$$x_m \approx 6.77\,\Gamma^{1/4},\ x_u \approx 5.45\,\Gamma^{1/4},\ x_2 \approx 4.6\,\Gamma^{1/4},$$
$$x_\ell \approx 4.05\,\Gamma^{1/4},\ \Gamma = \Pi_0/N^3 \qquad (19)$$

follow for the mean value $\sigma = 0.0088$ found from experiments in the self-similar section. The formula for x_m from (19) describes well the data of small model experiments [10] on the maximal height of rise of freely convective jets in a stably stratified medium.

Let us estimate the conditions constraining the applicability of (15) and (19). Since these expressions are obtained under the assumption of realization of the self-similar flow mode in a floating jet at low altitudes, then in conformity with (11) they will be valid when the following inequalities are satisfied:

$$\left(\frac{\Pi_0}{\sigma N^3 D_0^4}\right)^{1/4} \gg 2.0\,\mathrm{Fr}^{1/2}\left(\frac{\rho_0}{\rho_a}\right)^{1/4}, \quad \text{or} \quad u_0 N < 0.1 g \frac{\Delta\rho}{\rho_0} \quad (\text{for } \mathrm{Pr} = 0{,}6). \tag{20}$$

Condition (20) is not critical for strongly heated convective jets of products from fires or volcanoes [in the ISA the inequality (20) is satisfied for $T_0 - T_{a*} \approx 1000$ K even for a sonic initial efflux velocity $u_0 = 300$ m/sec). If (20) is not satisfied, the motion in the jet will conserve the forced convective nature up to the hanging and the maximal point of its rise in a stably stratified atmosphere will be determined by the magnitude of the initial dynamic momentum [11]:

$$x_m \approx 6\,(I_0/N^2)^{1/4}, \quad I_0 = \int_0^\infty ur^2\,dr = 1/8 u_0^2 D_0^2.$$

Besides (20), a constraint exists on the possibility of utilizing the vertical boundary-layer equations that can be written in the following approximate form for Pr = 0.6:

$$\frac{x_\ell}{D_0} = 4.05\left(\frac{\Pi_0}{\sigma N^3 D_0^4}\right)^{1/4} > 1, \quad D_0 < 4\,(\Pi_0/N^3)^{1/4}.$$

Using the relation between the buoyancy flux integral Π_0 and the thermal power of the source $Q_0 = 2\pi(p_a T_a)_* c_p \Pi_0/g = 2\pi\gamma p_* \Pi_0/[g(\gamma - 1)]$ for known $\gamma = 1.4$, $p_* = 1.013 \cdot 10^5$ Pa and $N = 0.0106$ sec^{-1}, we write the inequality presented above in the form

$$D_0 < D_* = 0.18\left(Q_0 \frac{p_* N_0^3}{p_\ell N^3}\right)^{1/4}, \tag{21}$$

where D_0 is in km, Q_0 is in MW, p_* and p_ℓ are the standard pressure in Pa at sea level and the actual pressure at the level of the source.

Spoilage of condition (21) denotes the necessity of taking account of the second equation of motion (in the coordinate r) in the original system. In the limit case ($D_0 \to \infty$) the source can be considered as distributed continuously over the area. The nature of the self-similar flow over it will be determined by the buoyancy flux density $\Pi \sim \Pi_0/D_0^2$, while the altitude of the hanging of the heated products is determined by the complex $(\Pi/N^3)^{1/2}$ [4].

IMPURITY EJECTION IN A STRATIFIED ATMOSPHERE

The substance flux (4) is conserved at short ranges from a constant power source when (11) is satisfied and the self-similar law (5) of the impurity distribution is realized, which for $\mathrm{Pr} = \mathrm{Sc}_j = 0.6$ in the variables (13) has the form

$$K_j = \frac{\varepsilon}{\varepsilon_{j*}} = \frac{2}{3\sqrt{3}} \exp(-\eta^2/2)\,\xi^{-5/3}, \tag{22}$$

where $\varepsilon_{j*} = P_{j_0}/(X_*^3 \sigma N)$ should be used as the characteristic concentration. Upon going over to the variables (18) the expression (22) takes the form

$$\frac{\varepsilon_j - \varepsilon_{j0}}{\varepsilon_{j0} - \varepsilon_{j\infty}} \quad \frac{\mathrm{Fr}_1^{4/3}}{4\frac{3}{1}\sqrt{3}\,\sigma}\,\tilde{x}^{-5/3} \exp(-\xi^2/(2\zeta^2)).$$

At altitudes comparable to X_*, the condition for conservation of the vertical flux of substance is spoiled and should be replaced by the integral impurity balance condition in the atmosphere

$$\int_0^\infty \int_0^\infty \varepsilon_j r\,dr\,dx = P_{j0}\,t, \quad P_{j0} \int_0^\infty u\varepsilon_j r\,dr,$$

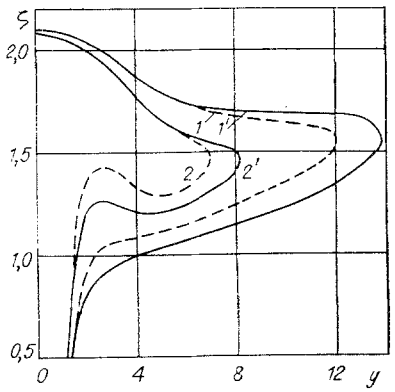

Fig. 2

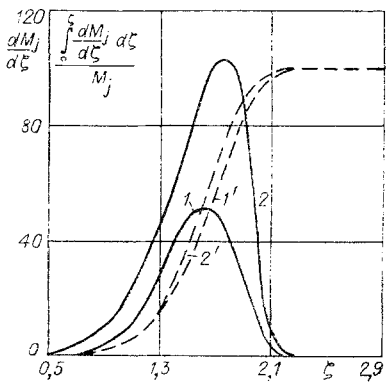

Fig. 3

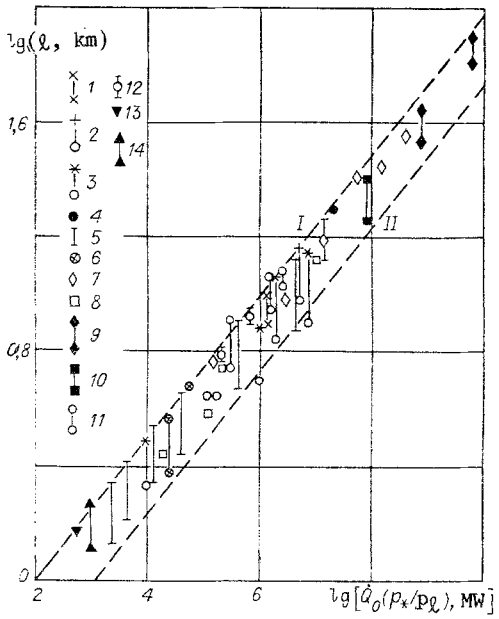

Fig. 4

which we write in the variables K_j, $y = r/(X_*\sqrt{\sigma})$, $\zeta = x/X_*$, $\tau = tN$ as

$$\int_0^{\infty}\int_0^{\infty} K_j y\,dy\,d\zeta = \tau.$$

Therefore, near the permanently acting source in a floating jet a stationary self-similar impurity distribution law (22) is realized while at altitudes comparable to X_* the nature of the transport is substantially nonstationary and described in the dimensionless variables taken by the equation

$$\frac{\partial K_j}{\partial \tau} + \frac{\partial}{\partial \zeta}\frac{K_j}{y}\frac{\partial \Phi}{\partial y} - \frac{1}{y}\frac{\partial}{\partial y}K_j\frac{\partial \Phi}{\partial y} = \mathrm{Sc}_j^{-1}\left[\alpha\frac{\partial^2 K_j}{\partial \zeta^2} + \frac{1}{y}\frac{\partial}{\partial y}y\left(\beta + \frac{\zeta\Phi}{y^2}\right)\frac{\partial K_j}{\partial y}\right]. \qquad (23)$$

Here $\alpha = E_1/(NX_*^2)$ and $\beta = E_2/(NX_*^2\sigma)$ are dimensionless quasilaminar transport coefficients in the vertical and horizontal directions (it is assumed that the kinematic viscosity along the radial coordinate equals the sum $E_r = E_2 + \sigma\Psi x/r^2$, and along the vertical $E_x = E_1$, where E_2 and E_1 are constants).

Equation (23) was solved numerically for $\mathrm{Pr} = \mathrm{Sc}_j = 0.6$ by using a modified scheme with differences opposite to the flux for a function Φ given from (15) and $\beta = 0.001$, $\alpha = 0.01$. Given as an initial condition for $\tau = 0$ was $K_j = 0$, while the boundary conditions had the form $\partial K_j/\partial y = 0$ for $y = 20$, $y = 0$ and $\partial K_j/\partial y = 0$ for $\zeta = 3$. For $\zeta = 0.5$ in the lower half-plane, a self-similar distribution was given for K_j in (22).

TABLE 2

Notation in Fig. 4	Source	Phenomenon	Power, MW (focus size, column altitude)	Remarks
1	[12]	Model of a fire in Hamburg, 1943	$1.4 \cdot 10^6$ (x_m = 8-10 km)	Average convective jet model
2	[13]	Model of an urban fire	$4.0 \cdot 10^6$ (R_0 = 4 km, $x_m \approx 15$ km)	Three-dimensional computation. Partially unstable stratification, $p_*/p_\ell \approx 1.2$. Taking account of wind and water vapor condensation. Upper point is jet edge, lower is position of maximum, dM_j/dx.
3	[14]	Fire model:		
		Long Beach, 1958	$1.0 \cdot 10^4$ (R_0 = 0.5 km, x_m = 3.2 km)	Two-dimensional computation. Without wind and condensation.
		Hamburg, 1943	$1.7 \cdot 10^6$ (R_0 = 2 km, x_m = 12 km)	
		Model city	$1.1 \cdot 10^6$ (R_0 = 5 km, x_m = 8 km)	Three-dimensional computation with wind and condensation. Lower point is maximum dM_j/dx.
4	[15]	Model focus	$2.0 \cdot 10^7$ (R_0 = 5 km, $x_m \approx 21$ km)	Three-dimensional computation in ISA without wind and condensation.
5	[16]	Floating jet	$2.6 \cdot 10^3$-$1.4 \cdot 10^7$ (R_0 = 0.09-2.8 km)	Average model. Numerical counting. Upper point is N = 0.0097 sec^{-1}; lower is N = 0.018 sec^{-1}.
6	[17]	Field experiment	$5.0 \cdot 10^4$ (20 ha square, x_m = 5 km)	
			$3.0 \cdot 10^4$ (12 ha, x_m = 3.8-2.8 km)	Upper point, slightly unstable stratification; lower, stable.
7	[18]	Volcanoes:		Δx_m, altitude of jet rise above crater apex; H, apex level [25].
		Sierro Negro, 2/5/72	$1.1 \cdot 10^5$ (Δx_m = 6 km)	H = 4470 m, p_*/p_ℓ = 1.74
		Agung, 5/16/63	$2.0 \cdot 10^6$ (Δx_m = 10 km)	H = 3150 m, p_*/p_ℓ = 1.47
		Fuego, 9/14/71		H = 3740 m, p_*/p_ℓ = 1.59
		Gekla, 5/5/70	$1.2 \cdot 10^7$ (Δx_m = 16 km)	H = 1500 m, p_*/p_ℓ = 1.2
		Gekla, 3/29/47	$5.7 \cdot 10^7$ (Δx_m = 27 km)	
		Nameless, 3/3/56	$2.8 \cdot 10^8$ (Δx_m = 36 km)	H = 2800 m, p_*/p_ℓ = 1.41
		Santa Maria, 10/24/02	$1.1 \cdot 10^8$ (Δx_m = 28 km)	H = 2500 m, p_*/p_ℓ = 1.35
8	[19]	Gekla, 5/5/70	$8.5 \cdot 10^6$ (Δx_m = 13.5 km)	
9	[20]	Nameless, 3/30/56	$5.9 \cdot 10^8$ (Δx_m = 35-44 km)	
		Krakatoa, 8/27/1883	$5.6 \cdot 10^9$ (Δx_m = 70-80 km)	H = 813 m, p_*/p_ℓ = 1.11
10	[23]	St. Helens, 5/18/80	$6.0 \cdot 10^7$ (Δx_m = 18-25 km)	H = 2975 m, p_*/p_ℓ = 1.43. Estimate of power according to acoustic gravitational wave energy

TABLE 2 (continued)

Notation in Fig. 4	Source	Phenomenon	Power, MW (focus size, column altitude)	Remarks
		Fires:		
8	[19]	Long Beach, 1958	$2.0 \cdot 10^4$ (x_m = 2.9 km)	
		Darwin River, 1971	$2.1 \cdot 10^5$ (x_m = 5.8 km) $1.1 \cdot 10^5$ (x_m = 4 km)	For different times
11	[21]	Air Force Bomb. Range	$1.2 \cdot 10^5$ (x_m = 4.6 km)	
		Tillamook County, 1933	$2.2 \cdot 10^6$ (x_m = 11-12 km)	
		Mack Lake Fire, 1980	$1.6 \cdot 10^5$ (x_m = 4.6 km)	
		Sierra Nat. Forest, 1961	$2.2 \cdot 10^5$ (x_m = 6-9 km)	
		Hamburg, 1943	$1.7 \cdot 10^6$ (x_m = 9-12 km)	
12	[22]	Sundance Fire, 1967	$5.0 \cdot 10^5$ (x_m = 9.2 km) $1.5 \cdot 10^5$ (x_m = 6 km)	H = 1500 m, p_*/p_ℓ = 1.2. Natural fire in mountains. Different times
13		Chernobyl atomic electric station fire	550 (x_m = 1.5 km)	
14	[24]	Field experiment	10^3 (x_m = 1.3-2 km)	Upper point, slightly unstable stratification; lower, stable.

Physically such a problem formulation corresponds to impurity diffusion in a given stationary velocity field from a permanently acting source. It is clear that such a task for the problem under consideration is approximate in nature since the diffusion source is switched on after velocity field buildup and not actually taken into account as the impurity loss during the time $\tau < \tau_* \approx 2\pi$. As the counting time ($\tau \gg \tau_*$) increases, the error induced here diminishes.

The result of the computation is illustrated in Figs. 2 and 3. The deformation of concentration isolines in time is represented in Fig. 2 in the coordinates ζ, y. The curves 1 and 1' correspond to $K_j = 0.275$ for $\tau = 38.18$ and 76.36 (1 and 2 h of real time), curves 2 and 2' to $K_j = 0.55$ for the same times. Given in Fig. 3 are dependences of the dimensionless linear impurity distribution density $dM_j/d\zeta \left(M_j = X_* N_0 \int_0^\infty K_j y\, dy / P_{j0} \right)$ on the altitude ζ for 1 and 2 h of real time (lines 1 and 2). The appropriate distributions of the relative total mass of substance taken out are represented in percentages for the same times by the lines 1' and 2' in Fig. 3. It is seen that after 2 h about 15% of the removable impurity is contained up to the lower edge $\zeta_\ell = 1.24$ of the hanging column of products, between the upper $\zeta_u = 1.67$ and lower edges is about 50% of the substance, and ~80% of the impurities between the maximal point of rise $\zeta_m \approx 2.1$ of the jet and the lower edge.

Therefore, the predominant fraction of the freely convective jet of impurities removed in a stratified atmosphere for times on the order of several hours is in a horizontal layer between the levels ζ_m and ζ_ℓ.

POWERFUL FLOATING JET IN A REAL ATMOSPHERE. COMPARISON WITH EXPERIMENT

The state of the atmosphere boundary layer (~1 km) influences weakly the maximal altitude of product rise for adequate thermal power of a turbulent floating jet. In this case, within the limits of the troposphere it is possible to consider approximately $N = 0.0106$ sec^{-1} = const and to use (19) for comparison with known experimental and computed data in the parameters of the hanging convective column of products above combustion and volcano foci acting in the continuous eruption mode.

It is useful to present the dimensional relationships following from (19) that connect the vertical coordinates of the characteristic points of the hanging jet to the thermal power of the source

$$x_m \approx 0.29\left(\dot{Q}_0 \frac{p_* N_0^3}{\rho_\ell N^3}\right)^{1/4}, \quad x_u \approx 0.24\left(\dot{Q}_0 \frac{p_* N_0^3}{\rho_\ell N^3}\right)^{1/4}, \quad x_\ell \approx 0.17\left(\dot{Q}_0 \frac{p_* N_0^3}{\rho_\ell N^3}\right)^{1/4} \tag{24}$$

(x in km, N_0 and N are Väisälä–Brunt coefficients in a standard and real atmosphere).

Results of experiments and theory are presented in logarithmic coordinates in Fig. 4. The lines 1 and 11 are the maximal x_m and minimal x_ℓ altitudes of the hanging cloud computed according to (24). The provisional notation, references to the sources of the data used in Fig. 4, and the characteristics of the foci of energy liberation under investigation are presented in Table 2. It is seen that the results of the elucidated two-dimensional analytic model agree satisfactorily (in the characteristic parameters of the convective jet rise) with both the prediction of the more general three-dimensional models realized numerically and with experiment. When condition (21) is spoiled (as occurred for part of the data [14], say), the heated products rose to a lower altitude than follows from (24).

According to (24), when (21) is satisfied, a heat source with power $\dot{Q}_0$ greater than $2 \cdot 10^6$ MW acting permanently in time will assure emergence of the upper edge of a freely convective jet beyond the troposphere limits (~11 km) into a normally stratified atmosphere.

The results represented can be used for both the analysis of the space–time pattern of atmosphere pollution by powerful freely convective sources acting a long time and to estimate the power of energy liberation in a focus by the measured altitude of the product rise.

LITERATURE CITED

1. M. I. Budyko, G. S. Golitsyn, and Yu. A. Izraél', Global Climatic Catastrophes [in Russian], Gidrometeoizdat, Moscow (1966).
2. Yu. A. Gostintsev, A. F. Solodovnik, et al., "Turbulent thermal in a stratified atmosphere," Izv. Akad. Nauk SSSR, Mekh. Zhidk. Gaza, No. 6 (1986).
3. B. R. Morton, G. I. Taylor, and J. S. Turner, "Turbulent gravitational convection from maintained and instantaneous sources," Proc. R. Soc., 234A, No. 1196 (1956).
4. Yu. A. Gostintsev, A. F. Solodovnik, and V. V. Lazarev, "On theories of aerodynamics, self-ignition, and combustion of turbulent thermals, vortex rings, and jets in a free atmosphere," Khim. Fiz., No. 9 (1982).
5. A. T. Onufriev, "Theory of vortex ring motion under the action of gravity. Rise of an atomic explosion cloud," Zh. Prikl. Mekh. Tekh. Fiz., No. 2 (1967).
6. Yu. A. Gostintsev and A. F. Solodovnik, "Powerful turbulent thermal in a stably stratified atmosphere. Numerical modeling," Zh. Prikl. Mekh. Tekh. Fiz., No. 1 (1987).
7. G. M. Makhviladze, O. I. Melikhov, and S. E. Yakush, "On numerical modeling of the rise of a turbulent thermal in an inhomogeneous compressible atmosphere," Izv. Akad. Nauk SSSR, Mekh. Zhidk. Gaza, No. 1 (1989).
8. Yu. A. Gostintsev, L. A. Sukhanov, and A. F. Solodovnik, "Stationary self-similar turbulent jet above a point concentrated-heat source," Izv. Akad. Nauk SSSR, Mekh. Zhidk. Gaza, No. 2 (1983).
9. H. Rouse, C. S. Yih, and H. W. Hamphreys, "Gravitational convection from a boundary source," Tellus, 4, No. 3 (1952).
10. M. S. Hossain and W. Rodi, "A turbulent model for buoyant flows and its applications to vertical buoyant jets," in: Buoyant Jets and Plumes, W. Rodi (ed.), Pergamon, Oxford (1982).
11. E. J. List, "Mechanics of turbulent buoyant jets and plumes," in: Buoyant Jets and Plumes, W. Rodi (ed.), Pergamon, Oxford (1982).
12. G. F. Carrier, F. E. Fendell, and P. S. Feldman, "Big fires," Combust. Sci. Technol., 39, No. 1 (1984).
13. W. R. Cotton, "Atmospheric convection and nuclear winter," Am. Sci., 73, No. 3 (1985).
14. J. E. Penner, L. C. Haselman, and L. L. Edwards, "Buoyant plume calculation," AIAA Paper No. 85-0459, New York (1985).
15. G. A. Hassing and M. Rosenblatt, "Firestorm formation and environmental characteristics after a large-yield nuclear burst," Proc. 17th Asilomar Conf. on Fire and Blast Effects of Nuclear Weapons (Livermore Nat. Lab. Report) (1983).
16. N. I. Vul'fson and L. M. Levin, "Investigation of meteor track jet propagation in a cloudy medium in application to active actions," Tr. Inst. Prikl. Geofiz., No. 46 (1981).
17. T. Y. Palmer, "Convection columns above large fires," Fire Technol., 11, No. 1 (1975).

18. S. A. Fedotov, "Estimates of ash and pyroclastics removal by volcanic eruptions and fumaroles by the altitude of their jets and clouds," Izv. Akad. Nauk SSSR, Vulkanolog. Seismolog., No. 4 (1982).
19. P. S. Manins, "Cloud heights and stratospheric injections resulting from a thermonuclear war," Atmos. Environ., 19, No. 8 (1985).
20. G. S. Gorshkov and G. E. Bogoyavlenskaya, Nameless Volcano and Singularities of Its Latest Eruptions 1955-1963 [in Russian], Nauka, Moscow (1965).
21. The Effects on the Atmosphere of a Major Nuclear Exchange, Nat. Res. Council, National Academy Press, Washington, D.C. (1985).
22. H. E. Anderson, Sundance Fire: An Analysis of Fire Phenomena, Paper INT-56, U.S. Dept. Agriculture, Forest Service Res., St. Louis (1968).
23. Yu. A. Gostintsev and Yu. V. Shatskikh, "On the mechanism of longwave acoustic perturbation generation in the atmosphere by the floating cloud of explosion products," Fiz. Goren. Vzryva, No. 2 (1987).
24. B. Benech, "Experimental study of an artificial convective plume initiated from the ground," J. Appl. Meteorology, No. 15 (1967).
25. V. A. Aprodov, Volcanoes [Russian translation], Mir, Moscow (1982).

EFFECT OF PRESSURE ON THE EXCHANGE OF ENERGY IN A VORTEX TUBE

V. I. Kuznetsov

UDC 533.601.16

In a number of works [1, 2] it has been noted that the thermal efficiency of vortex tubes only depends on the level of gas expansion and it does not depend on the overall pressure at the inlet to a tangential nozzle (with a constant temperature for gas stagnation and the weight fraction of cold flux μ). Theoretical conclusions have been confirmed by experiments with overall pressure at the inlet to a vortex tube greater than atmospheric ($p_{*+} \geq 10^5$ Pa). Although from experiments [1] it followed that a reduction in overall pressure ε leads to a certain reduction in thermal efficiency, it was assumed that pressure level does not play a role in vortex-tube operation. From analysis of a mathematical model for the process of energy separation for gas in a vortex tube [3] it follows that the thermal efficiency depends on kinematic viscosity coefficient which, in turn, is a function of overall gas pressure at the inlet to a tangential nozzle. In addition, the Rank effect should be reduced both with a turbulent and with a laminar regime for gas movement.

The aim of this work is experimental verification of the effect of overall gas pressure at the inlet to a vortex tube on its thermal efficiency (with constant T_{*+}, μ, and $\varepsilon = p_{*+}/p_{--}$) with laminary or turbulent regimes for gas movement in an energy separation chamber.

In order to obtain a laminar regime it is necessary to reduce the Reynolds number. This may be done without changing ε as a result of increasing the kinematic viscosity coefficient ν which depends strongly on pressure and grows with a reduction of it. Therefore, experiments were performed in a vacuum unit (Fig. 1) which consists of a valve 1, filter 2, water trap 3, receiver 4, nozzle block 5, inlet tangential nozzle of rectangular shape 6, energy separation chamber 7, alignment apparatus 8, valve 9, heated gas receiver 10, diaphragm 11, through which cooling air emerges, cooled-air receiver 12, pipelines 13 and 14 for removing the heated and cooled air from the vortex tube to vacuum unit 15. Air is discharged to atmosphere from the vacuum unit.

Overall pressure at the inlet to the vortex tube was controlled by means of a valve and a laminar or turbulent air-movement regime was established. Existence of flow pulsation (air-movement regime) was monitored by three strain gauges with consecutive readout in a mirror-galvanometer oscillograph. Strain gauges were placed at the inlet to the tangential nozzle, on the wall of the energy separation chamber ahead of the valve, and on the diaphragm.

Omsk. Translated from Zhurnal Prikladnoi Mekhaniki i Tekhnicheskoi Fiziki, No. 4, pp. 72-74, July-August, 1989. Original article submitted July 13, 1987; revision submitted May 25, 1988.

0021-8944/89/3004-0577$12.50